

Effectiveness of Combination Packages for HIV-1 Prevention in Sub-Saharan Africa Depends on Partnership Network Structure: A Mathematical Modeling Study

Supplementary Technical Appendix

1 INTRODUCTION

This supplementary appendix describes the mathematical model structure of the accompanying paper in more detail. Given our study's use of primary empirical data to parameterize our models, we also provide further detail on the behavioral data underlying the network model.

The mathematical models presented in this paper are agent-based microsimulation models in which uniquely identifiable sexual partnership dyads are simulated and tracked over time. This partnership structure functions through the use of temporal exponential-family random graph models (ERGMs), described in detail below. In addition to this dynamic network simulation, the larger epidemic model includes demography (entries, exits, and aging), inter-host epidemiology (disease transmission), intra-host epidemiology (disease progression), and clinical epidemiology (disease diagnosis, treatment initiation, and adherence). Individual attributes related to these processes are stored and updated in discrete-time over the course of the simulation.

Computationally, this model was programmed and executed in the R and C++ languages using *EpiModel* [<http://epimodel.org/>], software developed by the authors for the purpose of simulating complex network-based mathematical models of infectious diseases, with a primary motivation for HIV and other sexually transmitted diseases. *EpiModel* is part of and depends on *Statnet* [<http://statnet.org/>], a suite of software in R that provides tools for the representation, visualization, and statistical analysis of arbitrarily complex network data.¹

Our current modeling study presented here extends the general *EpiModel* software to incorporate HIV-specific elements not part of the core software package. These extensions are available as a stand-alone R package, *EpiModelHIVhet*, currently available for download on Github [<http://github.com/statnet/EpiModelHIVhet/>].

2 PRIMARY DATA

Unlike many mathematical models for HIV, our models uses rich socio-behavioral data on dynamic contact network structures that were collected specifically for the parameterization of these models.²

The empirical study that formed the basis of model parameters was called the *Migration & HIV in Ghana (MHG)* study. MHG was a cross-sectional study of sexually active adults in Agbogbloshie, Ghana in 2012. Agbogbloshie is an urban slum area in the capital city of Accra; it was selected as a study site based on its hypothesized high-risk profile and lack of prior epidemiological research in the community.

2.1 Design

The empirical MHG study design has been described in detail.³ Briefly, MHG used a two-stage cluster randomized sampling scheme to obtain a probability sample of the population. Starting with an area census, we first randomly selected households with probability proportional to household size, and then randomly selected one adult household member. Given differences in household size, a weighting scheme was employed to account for differential inclusion probabilities. Eligibility criteria to participate were current residence in the selected household, age 18 to 49 years, and lifetime history of consensual sexual intercourse. The Institutional Review Boards of the University of Washington and University of Ghana approved all study procedures.

2.2 Measures

Trained field staff administered a standardized structured survey and drew blood serum via finger stick for a diagnostic HIV-1/2 test. The survey focused on demographics, migration and travel, and sexual behavior. For sexual behavior, summary data were collected on the number of lifetime sexual partners, past-year partners, and past-year partners with whom condoms were not always used. We used an event-history calendar to collect detailed partnership data for up to three partners within the prior year, with data collected for each month during that period.⁴ For each partner, data included the duration of the partnership and monthly information on the number of total and unprotected sexual acts.

The HIV testing platform consisted of collecting dried blood spots in the field on standard filter paper and maintained in refrigerators before delivery to the Department of Virology, Noguchi Memorial Institute for Medical Research, University of Ghana for processing. Serum was tested on the INNO-LIATM HIV-1/2 test platform (Innogenetics, Belgium), shown to have good sensitivity and specificity for diagnosis and HIV type differentiation. All subjects who tested were asked to return in one week to receive their test results, which were provided by a trained nurse counselor. HIV-infected subjects were referred to medical care and other necessary health services.

3 SEXUAL NETWORK MODEL

At the center of our mathematical model for HIV transmission dynamics is the dynamic network structure, which is comprised of the HIV-related sexual contacts that individuals make and break

over time. A dynamic model for the formation and dissolution of sexual partnerships based on the empirical data described above was estimated and simulated with the statistical methods of exponential-family random graph models (ERGMs).⁵ ERGMs provide a foundation for a statistically principled simulation of local and global network structure given a set of target statistics from empirical data. In this section, we describe the statistical and mathematical framework of this approach, and then discuss the specific parameterization of the network model in this study.

3.1 Mathematical Framework

Temporal ERGMs consist of a formation model and a dissolution model. The formation model governs how two actors not previously connected within the network pair, and the dissolution model influences how two currently paired actors dissolve their dyad. In the formation model, the probability of observing a set of Y relations among n actors given a set of attributes is expressed as:

$$P(Y = y|n, X) = \exp\left(\frac{\theta'z(y)}{\kappa(\theta, n, X)}\right)$$

where $z(y)$ are a set of network statistics, and θ are coefficients to be estimated from the model. The denominator is a normalizing constant, κ , which is not analytically estimable given the potential number of network configurations. Therefore, simulation-based estimation methods using Markov-Chain Monte-Carlo (MCMC) sampling are used to obtain maximum likelihood estimations for θ given the set of network statistics, z , and the observed data, y .⁶

Network statistics may be arbitrarily complex, and fall into two main classes: dyadic-independent and dyadic-dependent statistics.⁵ Independent statistics are those in which the probability of dyad formation between any two nodes, i and j , does not depend on the existence of ties from i and j to other nodes (i.e., persons) in the network. Examples include the propensity for mixing by sex (i.e., heterosexual mixing) or age-based homophily (i.e., choosing a similarly aged partner). In contrast, dependent statistics are those in which the probability of the tie between i and j depends on the presence of any ties from those two nodes to other nodes in the network. An example is degree, which is the number of active ongoing ties for each node. The probability of forming a tie with a new potential partner may be hypothesized to depend on the existence of ties already in existence.

Dynamic network models also include a dissolution component that predicts the network statistics associated with ties dissolving conditional on their existence.⁷ In the current statistical methods, the formation and dissolution models are said to be separable within each time step: for any node the process of tie formation is independent of tie dissolution within a time step, but dependent over time. The implications of this assumption are that the size of the time step must be sufficiently minimized to reduce the effects of the within-step competing risks.

The dissolution model may be estimated a number of ways. In this current study, we use the “Edges Dissolution” approximation method of Carnegie et al.,⁸ in which a static ERGM was fit and the formation coefficients statistically adjusted to account for edge dissolution. This method was chosen for computational tractability compared to fitting full temporal ERGMs. The two methods are implemented in the *EpiModel* software and described in greater detail on our tutorials (online at: <http://epimodel.org/>).

With the network simulation method implemented in *EpiModel*, a complete network need not be observed. We therefore used our egocentric network data, from the MHG Study, to query localized network measures (e.g., attribute-based homophily and degree). The MCMC-based simulation used for network model estimation is also used for the simulation of complete networks with features stochastically varying around target statistics from the data. Our specific model parameterization is provided below, but the egocentric framework is discussed in more detail elsewhere.⁹

Finally, for the dynamic simulations two adjustment methods were used to account for the changes to the population composition over time. The first adjustment was to preserve mean degree (i.e., the average number of partners per person at any time) given fluctuations in population size with births and deaths. The offset method of Krivitsky⁹ holds this mean degree constant, a reasonable assumption for HIV/STI epidemic models. This adjustment also allowed the data from the original MHG study sample to be projected up to a network size representing the size of the underlying population: we started all simulations with a network size of 10,000 nodes, which grew slightly over time with demographic trends. This adjustment is automatically calculated and applied in the *EpiModel* software.

The second coefficient adjustment method was to account for the presence of deaths or exits from the network as an exogenous competing risk for partnership dissolution, on top of the endogenous rates of partnership dissolution observed in the data. Since the empirical data were cross-sectional, we did not observe mortality rates to be able to partition the partnership dissolution into these two components. Therefore, we used an adjustment of the dissolution coefficients whereby the probability of tie persistence (the complement to tie dissolution) was adjusted upward to account for the competing risk from mortality. This adjustment is also automatically applied in *EpiModel*.

3.2 Parameterization

The contact network model was parameterized from empirical data collected in the MHG study described above. This section provides information on the structure of the formation and dissolution models, how the data were estimated, and methods for dynamic model calibration.

Formation Model. Given the aims of this study our network models were formulated to capture the unique sex and age-based mixing structure and degree distributions in a heterosexual population in Sub-Saharan Africa (SSA). The network statistics were directly estimable via egocentric inference from the empirical cross-sectional data in MHG. The formation model included the following elements:

1. **Mean degree.** The overall number of dyads observed in the cross-sectional data was modeled with an edges term in the ERGM. This term is commonly used like an intercept in a generalized linear model, so that the remaining coefficients are interpreted in reference to its value. The number of edges in the model was based on a calculation of cross-sectional mean degree at the day of the study. As noted, the coefficient was adjusted to account for differences in the observed study sample and the simulated network size, preserving the mean degree. In the data, the observed mean degree was 0.91 overall, corresponding to an expected 4,544 edges in a network of size 10,000 (this was the starting network size used in our simulations).
2. **Heterosexual mixing.** This model is designed to study purely assortative mixing between women and men in the population (i.e., only heterosexual HIV spread). This was both a simplifying assumption of the model, and also reflecting the fact that no same-sex partnerships were observed in MHG. At the time of the study, same-sex activity was illegal in Ghana, so there was strong bias against study participants subject reporting on this behavior. In the model, we parameterized heterosexual mixing as an offset term for the nodematch network statistic for the attribute of sex. This involved fixing the coefficient at a value of negative infinity so that the term was not estimated in the model fitting procedures. Simulations from the model fit were consistent with this constraint.
3. **Degree distribution by sex.** Without degree terms in the network model, the degree distribution (the number of persons with a momentary degree of 0, 1, 2, and so on) would follow a Poisson distribution with the rate parameter equal to the product of mean degree and population size. In our data, we observed many fewer concurrent nodes (persons with a degree of 2+) than expected under this null model, and furthermore, the degree varied largely by sex: concurrency was much more common in men than in women. To capture this, we included terms for the number of nodes with concurrency, differential by sex of the node. The baseline values for this were 17.8% for men and 2.8% for women. These were transformed into a number of concurrent nodes given the population sizes of men and women, and modeled using the concurrent(by = "male") statistic in ERGM.
4. **Degree constraint.** As described in prior reports,³ our data collection tool was capped at the last three partners in the past year, primarily to reduce response fatigue. This would miss a certain proportion of respondents who had a high momentary degree (4+). However, the

cumulative number of partners was greater than 3 in only 7% of men and <1% of women; the momentary degree would typically be much less than even this. Because of this constraint in the data collection, this influences the calculation of the mean degree and other degree statistics. Therefore, we used a constraint term in the model to cap the number of ongoing partners at any one time at 3.

5. **Sex-structured age homophily.** Typical of heterosexual mixing,¹⁰ our study population tended to select sexual partners similar in age (age homophily), but with a sex-structured directionality. This directionality was such that men were on average 5.38 years older than women. To model this, age was included as a continuous attribute with values following the empirical data. A new ERGM term was coded using the `ergm.userterms` software package to parametrically model the absolute difference in ages with sex-structured directionality.¹¹ This network statistic includes both an offset value (5.38 years) and a residual sum after the offset that controls the variance of the distribution. Model diagnostics were checked to ensure that the offset mean and variance were preserved over changing age distributions that reflected demographic trends. This new ERGM term, `absdiffby`, is included in the *EpiModelLHIVhet* extension software package.

Dissolution model. In contrast to the formation model, the dissolution model includes only one network statistic, which is a function of the average duration of partnerships observed in MHG. There have been several methods used to parameterize this statistic.¹² In the egocentric network sampling framework supported by *EpiModel*, one must estimate the coefficients for the formation model conditional on coefficients for the dissolution model. Therefore, the dissolution model coefficients are analytically calculated and entered as a fixed offset values that control the rate of partnership dissolution.

In our approach, we use Kaplan-Meier methods to estimate the survival distribution of the empirical partnership durations from MHG.¹³ The assumed parametric model for partnership duration (time to dissolution) was therefore a homogenous exponential dissolution. In general, this model was consistent with the empirical form from the data although resulted in a slightly higher than average number of medium-length partnerships. Additional methodological work is underway to build in hyperexponential distributional forms allowing for heterogeneity in partnership types.

In the MHG dataset, the start and end dates of up to the three last partnerships in the prior year were recorded, by calendar month and year. To obtain daily intervals, we sampled from days of the month with a uniform distribution to obtain an imputed starting and ending date. All partnerships that were qualitatively described as "one-offs" by the study participant were coded as one day in duration. Partnerships that had not ended on the date of the study were right-censored, whereas the

duration for the remaining partnerships was considered fully observed. The KM survival curve was available down to the 68th percentile (only 32% of queried partnerships had dissolved by the study date). The network model dissolution coefficient is expressed as a λ coefficient in a geometric distribution. We estimated λ for a geometric distribution that matched the 75% percentile of the observed KM survival curve. The 75th percentile was 1,978 days, which matched a λ parameter of 1/1453 days. Therefore, the average partnership duration based on the empirical data was estimated at 1,453 days or 3.97 years.

This duration coefficient was used as the *only* calibration parameter in our epidemic model. In order to fit the model results to HIV prevalence observed in MHG, the coefficient was adjusted downward. With no adjustment, the endemic HIV prevalence was too low relative to observed data, and therefore we adjusted the mean of 1,450 days to 1,124 days (or 3.08 years) to calibrate. This 22% reduction was theoretically justified based on the comparison of the observed duration data to the homogenous geometric distribution probability mass function of the original estimated mean duration. The geometric distribution with that single homogenous parameter underestimates the number short-duration partnerships and overestimates the number of long-duration partnerships. For example, we observed 28.6% and 9.6% of partnerships were under 1 years and 1 month of duration, respectively. The expected percentiles given the original λ above are 22.3% and 2.0%, respectively.

Additionally, this 3.08-year average partnership duration reflects an average number of lifetime sexual partners of 10.1 given a modeled sexual lifespan of 35 years. This closely reflects the best estimation of the average number of lifetime partners based on cumulative partnership data we observed in MHG (9.6 lifetime partners). Therefore, the calibration parameter is both theoretically and empirically justifiable. This justification may not necessary hold in other populations where the mean degree or average partnership duration are different.

4 DEMOGRAPHY

In this model, there are three main demographic processes: entries, exits, and aging. Entries and exits are conceptualized with respect to flows to the sexually active population. This is the point at which persons become at risk of infection via heterosexual transmission, and we model these flows as starting at an age after birth and potentially ending at an age before death.

4.1 Sexual Entry/Birth

All persons enter the network at age 18, which was the lower age bound of the MHG study student eligibility criteria.³ The number of new entries at each time step is a proportional function of the current population size at that time step. This entry rate parameter was fixed so that the average annual growth rate of the population was 1% per year in our dynamic simulations after a burn-in period. In Section 9, we describe the difference between the burn-in and research simulations. The

number of entries at each time step was simulated by drawing from a series of binomial distributions with the probability parameter set to the entry rate, and the length of the series equal to the population size.

Incoming nodes were randomly assigned a sex and, for males, a circumcision status. The probability of assignment as male sex was based on a parameter to a draw from another binomial distribution series that stochastically maintained the sex ratio distribution at the outset of the simulation. This initiation sex distribution was 54.9% female and 45.1% male, which was estimated from the MHG data. The sex ratio imbalance likely arises from the high circular migration of men within the community.¹⁴ The specified level of circumcision in the base model was that observed among men in the MHG study, 90%, similar to other West African countries.¹⁵ The circumcision status was also randomly assigned at entry with a binomial series. Counterfactual models for this study varied that probability for incoming nodes.

4.2 Sexual Exit/Mortality

All persons exit the network by age 55, either from death or assumed cessation of sexual activity. The upper limit of age 55 was modeled deterministically for everyone in the network. The exits due to death were stochastic processes based on natural (non-HIV) and HIV-related causes before that age. Background mortality was modeled with age-specific and sex-specific mortality rates derived from the World Health Organization's demographic life tables for Ghana.¹⁶ These tables are included as data within the *EpiModelHIVhet* package.

Life table data provide the probability of death by age and sex for the population for the year 2010, closest to the date of our MHG empirical study. The mortality rates were then applied to active persons within the network through a stochastic process by drawing from a binomial series for each eligible person with a probability corresponding to that person's risk of death related to his/her age and sex. Disease-related mortality, was modeled based on clinical disease progression, described in Section 5 below.

4.3 Aging

The aging process in the population was linear by time step for all active nodes. The unit of time step in these simulations was one week, and therefore, nodes were aged in weekly steps between the minimum and maximum ages allowed (18 and 55 years old). Nodes who exited the network from death were no longer active and their attributes were no longer updated.

5 INTRAHOST EPIDEMIOLOGY

Intrahost epidemiology includes those processes related to disease progression within infected persons. The two main components of progression within the HIV context are CD4 count and HIV

viral load.¹⁷ Whereas the behavioral and demographic parameters were derived from the MHG study and related Ghana data, parameterizing intrahost epidemiology depends on clinical data from large external cohort studies and clinical trials, referenced below.

5.1 CD4 Progression

Persons have a CD4 count assigned at infection. Post-infection, that count declines naturally in the absence of anti-retroviral therapy (ART) and rises with successful ART. The underlying model for the decline follows Pantazis and colleagues, summarizing a meta-cohort of Africans.¹⁸ This model has a non-linear decline in CD4 count based on age at infection and sex within Sub-Saharan Africa. Women have a higher baseline CD4 compared to men, and the rate of decline is faster when persons are infected at an older age. The decline is non-linear as the slopes are calculated on the scale of square roots of CD4 count.

Supplemental Table 1 shows example values of the base CD4 count at infection and then the years it takes to reach certain threshold values of 350, 200, and 100 cells. As noted, women have a higher base value and progress to AIDS more slowly than men. Persons infected at younger ages will progress more slowly than those infected at older ages across sex.

Supplemental Table 1. CD4 Clinical Model

	Base Value	Years to Threshold		
	<i>Base CD4</i>	350	200	100
Male				
<i>Age Infected</i>				
25	518.4	3.53	7.50	11.10
35	518.4	3.24	6.90	10.22
45	518.4	2.73	5.79	8.57
Female				
<i>Age Infected</i>				
25	570.3	4.50	8.47	12.07
35	570.3	4.13	7.79	11.10
45	570.3	3.47	6.54	9.31

Disease-induced mortality is a stochastic process when the CD4 crosses a late-stage AIDS threshold. Similar to Eaton and Hallett,¹⁹ we model this threshold level at a count of 50 CD4. Once persons hit that threshold, disease-related death occurs on average within one year. This is parameterized by a series of binomials draws with probability equal to an expected mortality in one year. Since this is a stochastic process of geometrically distributed waiting times, persons may not

randomly die before they reach a CD4 of 0, but that lower limit is enforced as a deterministic process.

5.2 HIV Viral Load

Following prior approaches,¹² we parameterize changes in HIV viral load to account for the heightened viremia during acute-stage infection,²⁰ viral set point during the long chronic stage of infection, and subsequent rise of VL at clinical AIDS towards disease-related mortality. A starting viral load of 0 is assigned to all persons upon infection. From there, the natural viral load curve is fit with the following parameters.

Post-infection, it takes 14 days to reach peak viremia,²¹ at a level of $6.7 \log_{10}$.^{21,22} From peak viremia, it takes 107 days to reach viral set point,²³ which is at a $4.5 \log_{10}$ level.^{21,22} The total time of acute to chronic-stage infection will depend on CD4 progression using the model specified above. Rise of viral load begins during AIDS-stage infection, which occurs when the CD4 reaches a threshold of 200. This again follows the Pantazis disease progression model.¹⁸ For men infected at age 45, that will occur 5.8 years after infection; for women infected at age 25, it will occur after 8.5 years.

During this late-stage infection period, viral load will rise from the set point of $4.5 \log_{10}$ to a maximum of $7 \log_{10}$.¹⁷ The time it takes to reach this maximum is also a function of the CD4 slope, and with the time it takes to transition from a CD4 of 200 to a CD4 of 50, at which point late-stage AIDS with a high probability of mortality will occur.¹⁹ These transitions are deterministic for all individuals. The VL trajectory is for ART-naive persons. The influence of ART on this trajectory is described below.

6 CLINICAL EPIDEMIOLOGY

Clinical epidemiological processes refer to disease diagnosis and treatment. In our model, diagnosis and treatment occur simultaneously based on the CD4 level of the respondent. This follows the empirical research of Collini et al. in Ghana that provides the mean and standard deviations of CD4 upon treatment initiation, which were 120 and 88 respectively.²⁴ This assumption that there is no waiting time between diagnosis and treatment implies that individuals do not change their sexual risk behavior between the two events; there are no representative data on this for Ghana.

6.1 Antiretroviral Therapy (ART) Initiation

Upon infection, each person is assigned a CD4 count at which they will initiate ART. This is drawn from a negative binomial distribution with mean and standard distribution parameters specified from Collini above. Based on their statistical tests, that study implied that the CD4 values were normally distributed. However, it was necessary to re-express this as a negative binomial statistical

distribution because the parameter values (120 mean; 88 SD) for a normal distribution result in 9% of the density below 0. We further scaled the standard deviation parameter for the negative binomial to 40 because the original value resulted in a tail where a considerable portion of the mass was above a threshold initiation value. Sensitivity analyses showed this had no substantive impact on the results.

The threshold ART initiation CD4 count for Ghana was based on the country's national AIDS policy at the time of the study, in which persons could begin treatment at or below a CD4 of 350. Therefore, the draw for the individual-level count of when to initiate ART was capped at this 350 CD4 count value. Individuals could not initiate therapy above this count, and the average count at ART initialization followed the mean parameters.

There was an overall treatment coverage enforced among those reaching below their threshold values. Treatment coverage was expressed as the proportion of treatment-eligible persons (those with a CD4 under 350) had ever initiated treatment. While population-level data on this for Ghana are not available, one report estimates that this current level is 30%, and we used this as the base parameter in the model.²⁵ Persons were allowed to initiate treatment, therefore, only if their current CD4 level had reach their targeted initiation value and less than 30% of eligible persons were currently "on ART," even if their adherence to ART had lapsed.

6.2 ART Adherence

Adherence to ART was modeled to achieve an overall level of viral suppression among those who had ever initiated ART. Since ART adherence over the disease history is a complex dynamic process, with uncertainty in how persons adhere to ART across disease stages, we used a back-calculation method in which we targeted that 80% of those who had initiated ART were virally suppressed. This is consistent with a recent UNAIDS analysis of viral suppression levels across Sub-Saharan Africa.²⁶

Modeling adherence in this way involved partitioning the on-treatment population into two groups: full adherers and partial adherers. Based on a meta-analysis of ART adherence that included many Sub-Saharan African countries, we set the full adherence proportion to 76% of the on-ART population.²⁷ Upon ART initiation, persons were assigned to the full versus partial adherence groups using a series of binomial draws with probability parameters set to this 76% value.

Full adherers remained on ART for the duration of their disease with no lapses. Sustained ART use conferred two clinical benefits: increased CD4 and decreased HIV viral load. Based on data from Collini from Ghana,²⁴ the rebound in CD4 was modeled as a linear daily increase in CD4 level, with the slope conditional on sex of the person. CD4 count for males increased at an average of 9.75 per month; for females it was 11.6 CD4 cells per month. For full adherers, the CD4 increased back

up to the level at initial infection, where it stayed for the duration of disease. ART was associated with a rapid and sustained decrease in HIV viral load,²⁸ from the person's current level to viral suppression, which we set at $1.5 \log_{10}$, just below the limits of detection ($1.65 \log_{10}$).¹²

Partial adherers cycled back and forth between ART use and non-use as a Markov process at each time step. The probability of cycling was calibrated to 50% at each time step, which resulted in the overall level of viral suppression of 80% among those who had initiated ART.²⁶ Cycling off treatment resulted the reverse immunological and virological phenomena as cycling on treatment: CD4 declined at the negative rate it increased on ART and viral load increased at the positive rate it decreased on ART.

7 INTERHOST EPIDEMIOLOGY

Interhost epidemiological processes simulate the HIV-1 disease transmission in this model. Disease transmission occurs between sexual partners who are active on a given time step. The transmission rate formally provided below is expressed as a rate per partnership per unit time, which was one week in our model. This section will describe how the overall rate as a function of the intrahost epidemiological profile of each member of a partnership, and behavioral features within the dyad.

7.1 Disease-Discordant Dyads

At each time step in the simulation, a list of active dyads is selected from among the nodes in the network. This “edgelist” reflects the work of the network model simulation, wherein partnerships form on the basis of nodal attributes like age and sex, as well as current degree up the constraint of three (see Section 3). Dyads are active at a specific time step if the terminus of that simulated edge is less than or equal to the current time step (right-censored). From this total edgelist, a disease-discordant subset is created by removing dyads in which both members are susceptible or both infected. This leaves those dyads that are discordant on HIV status (one susceptible and one infected partner). This is the set of potential partnerships over which disease may be transmitted at that time step.

7.2 Per-Act HIV Transmission Probability

Given an active discordant dyad selected from the current edge list, next needed is a per-act HIV transmission probability within that dyad. We use a statistical prediction model based on a recent study by Hughes et al. on transmissions within serodiscordant couples in chronic-stage infection.²⁹ Their model relates the per-act transmission probability to the HIV viral load of the infecting partner, as well as the sex, age, and circumcision status of the susceptible partner. Also incorporated in their full model are co-infection with other sexually transmitted infections like Herpes Simplex Virus-2 (HSV-2). Because we did not have individual-level data on STIs, we used the population-level means assumed in the Hughes study.

The core component of the statistical model is the non-linear relationship between the HIV viral load of the infecting partner and the transmission probability given a sexual act. The association is linear in \log_{10} VL, and therefore non-linear with respect to the outcome probability. The probability of transmission from an infected male partner with a \log_{10} VL of 2, 3, 4, 5, 6, for example, to a susceptible female partner aged 35 would be: 0.0001, 0.0002, 0.0005, 0.0015, and 0.0044. The full model is parameterized in the *EpiModel* *LHIVhet* function *hughes_tp* available in the software.

As noted, Hughes et al. estimated transmission probabilities only for chronic and late-stage infection, and therefore their model does not account for the increased risk of transmission during acute-stage infection above and beyond that predicted by the peak viremia during that period.²⁰ Similar to Eaton and Hallet¹⁹ and others modeling primary infection, we added a base multiplier of 5 onto the transmission probability if the infected partner was in the acute stage of infection. This brings the overall transmission probability during this stage in line with earlier predictions from Wawer³⁰ and Hollingsworth,³¹ which were better able to quantify the transmission probabilities during early infection.

7.3 Coital Frequency

The total number of sexual acts per partnership per unit time was modeled initially based on MHG study data, but we observed likely underreporting of acts based on the epidemic extinction in model simulations. Therefore, following similar mathematical models, we used per-partnership act rates based on data from Rakai, Uganda data.³⁰ Another key benefit of this data source is that it includes coital frequency variation by disease-stage, which was not available in MHG. In the absence of stage-specific rates, highly-infective AIDS-stage patients would likely drive much of the epidemic. The rates were 0.362 per partnership per day in early and chronic stage infection and reduced to 0.197 during AIDS-stage infection. With these rates, the total number of acts per partnership for that time step were then drawn from a Poisson distribution with the rate parameter set to that respective rate based on the disease stage of the infected partner.

Our initial model included parameters for coital dilution, which is defined as the reduction in per-partnership coital frequency when additional, concurrent partners are added. Under full dilution, persons have a fixed act budget that does not vary when additional partners are added. However, our previous work on the MHG study found minimal evidence for coital dilution in Ghana,³² similar to previous reports in SSA.³³

7.4 Condom Use

Condom use is typically ignored or conflated into the overall act rate in many mathematical models, but we separated it out based on our MHG Study data that 9% of acts were protected by condoms. To generate a number of protected and unprotected acts at each time step for each serodiscordant dyad, we drew from a Poisson distribution for the total number of acts, and then from a binomial

series for each act with a probability equal to the observed condom use. For the effect on transmission risk, we modeled condom use during sex associated with a 78% reduction in the risk of transmission per act, also derived from the Hughes per-act transmission probability model.²⁹

7.5 Transmission Rate

Given the elements above, the overall transmission rate per partnership per unit time is expressed as:

$$1 - [((1 - \tau * (1 - \omega))^{\alpha_p}) \times ((1 - \tau)^{\alpha_u})]$$

where τ is the base transmission probability, ω is the efficacy of condoms, α_p is the number of acts protected by condoms, and α_u is the number of unprotected acts. Therefore, the overall transmission rate is the 1 minus the product of probability of remaining susceptible due to protected acts and the probability of remaining susceptible due to unprotected acts. These transmission rates were independent across partnerships.

8 INITIAL CONDITIONS AND MODEL CONFIGURATIONS

To initialize the epidemic simulations, it was necessary to set initial conditions of demography and epidemiology from which the natural infectious disease dynamics would flow. For our baseline models, we initialized the prevalence at 1% in order to generate an endemic HIV prevalence and incidence close to the observed value for our data.

Among those initialized as infected, the time of infection was assigned by drawing from a geometric distribution with probability parameter equal to the average treatment-naive lifespan (roughly 12 years). Initial CD4 count and HIV viral load for those infected were based on the clinical model described above, with the main parameters determining the disease stage linked to age at infection and sex. All infected persons were initialized as undiagnosed and untreated infection, but persons meeting their individualized CD4 threshold for ART were then immediately started upon the simulation.

The time unit for all simulations was one week. The choice of unit in microsimulation models like these is a tradeoff between computational efficiency (longer time units takes less computation given a fixed calendar time period for simulation) and competing risks. The latter is a concern for discrete-time dynamic models, as multiple processes must occur “at” a specific time. The discrete-time representation is an approximation to continuous time, in which individual events occur at distinct times.³⁴ In our models, a one-week interval for simulation provided the best balance between the bias of competing risks and computational efficiency. Smaller-scale diagnostic simulations at daily time step intervals (not shown) did not yield different substantive outcomes.

In the MHG study population, there was a strong 1.22:1 female-male sex ratio. Typically in mathematical models stratified by sex, a balanced sex ratio is assumed, but we sought to preserve the proportional disparity that was reflective of sex-based differences in demographics, including death and migration. In our population, high rates of circular migration among men may have led to a selection bias for this sex.¹⁴ Although we did not simulate migration *per se* in the models, it is incorporated within the entry and exit rates along with this imbalanced sex ratio.

9 BURN-IN AND COUNTERFACTUAL SIMULATIONS

The prevailing method for mathematical models for HIV is to model a quasi-historical time series of an epidemic, which typically starts in the early 1980s. Modelers use either fixed behavioral and biological parameters estimated usually more recently than the epidemic onset, and assume they have remain unchanged over that time period.³⁵ These types of models require, for these and related reasons, parameters for partnership turnover that exceed nearly any population-level empirical data.³⁶ Other modeling studies use statistical approaches like Bayesian melding³⁷ to define a plausible range of values for such parameters over that period, and allow them to vary in order to match known epidemiological data on disease prevalence and incidence.³⁸

Neither approach would be suitable for our models: the fixed-parameter approach because it would be unreasonable to assume that individual behavior related to sexual risk have remained fixed at their current levels since the epidemic beginning. The Bayesian approach that allows parameter variation over time is undesirable because behavioral and clinical parameters are allowed to vary over multivariate distributions that may not ever match empirical data.

Our approach is to model the *current* state of the epidemic given *current* clinical and behavioral parameters. Therefore, the objective of the simulation is to reach a stable equilibrium point with respect to epidemiology after a burn-in period, and then to analyze results after that stationary distribution has been reached.¹² The burn-in period allows the initialization of the epidemic (e.g., the age distribution and disease prevalence) to not have direct influence on the outcomes under investigation. For the base model representing the epidemic in Ghana, we achieved equilibrium after approximately 50 “years” of simulation. That does not represent the actual time it takes to generate the observed epidemic, since many parameters have changed since those which we observed in more recent empirical data. Given the stochastic variability in the data, the goal was to generate and maintain a stationary distribution in HIV prevalence and incidence – that is, an endemic prevalence given the parameters for each model – across all disease simulations. For this study, we defined the equilibrium point for each parameter set of simulations as maintenance of population-level HIV prevalence within a margin of 0.1% across the final 1000 time steps (~ 20 years).

Our stochastic modeling approach represents HIV transmission as a random process in order to reflect uncertainty in both the input parameter values and also the mechanics of transmission system itself. According to stochastic theory, the actual prevalence of 4.7% in Accra, Ghana (itself observed with sampling error) was just one of many real-world epidemic possibilities, where a different random course of events could have led the epidemic to be larger or smaller even assuming the same circumcision rates, network structure, and other features. Summarizing the stochasticity, including the outliers, is central to this epidemic modeling framework. The distribution of model outputs, such as HIV prevalence, may be summarized in a number of ways, including the full distribution (shown in Figure S1 below), and also predefined intervals such as the interquartile range (see Table 1 of the main text). While the full distribution ranged from nearly 0% to 10% in the base model, the middle 50% of simulations (the interquartile range) was between 3.5% and 5.6%. On average, the model runs were in a steady equilibrium state, at the calibrated prevalence of 4.7%, even if the prevalence value deviated from that number or the slope of the prevalence curve was greater than the 0.1% in some individual simulations. Variation away from the observed prevalence does not indicate an overall poor model fit, only that the underlying system is capable of producing a wide range of outcomes given the inherent randomness in the model.

We used a total of 36 parameter sets. Circumcision prevalence started with the baseline 90% observed in the data, and then down to 10% in increments of 10%. We varied concurrency at four levels covering the levels observed across Sub-Saharan Africa. The starting base value, which we call *High*, equals a point prevalence of concurrency of 17.8% for males and 2.8% for females. The *Moderate*, *Medium*, and *Low* scenarios were equal to 75%, 50%, and 25% of the base values by sex, respectively.

For each parameter set, we conducted 250 simulations across 100 years of time. Each population started with a network size of 10,000 nodes. This is approximately the size of the population of Agbogbloshie in Ghana, but that was only a coincidence. Because the summary statistics reported here (prevalence and incidence) were measures scaled to the population size, the network size in the simulations should not impact the results in their expectation. In fact, when we used a starting network size of 5,000 instead of 10,000, there were no substantive changes in the results. As noted, it took approximately 50 years for the model burn-in period to complete. Therefore, we analyzed data from either the final time step, or an average over the final year of data in each simulation.

10 SUPPLEMENTAL FIGURES

Figure S1. HIV prevalence over burn-in and analysis time periods for the base model. The burn-in period lasts for the initial 50 years. Endemic equilibrium HIV prevalence level fit to seroprevalence data of 4.7%. Blue lines show results of 250 model simulations, and the red line shows the mean across all simulations. Summary model statistics derived from the final 100 time steps of each of the 36 simulation sets.

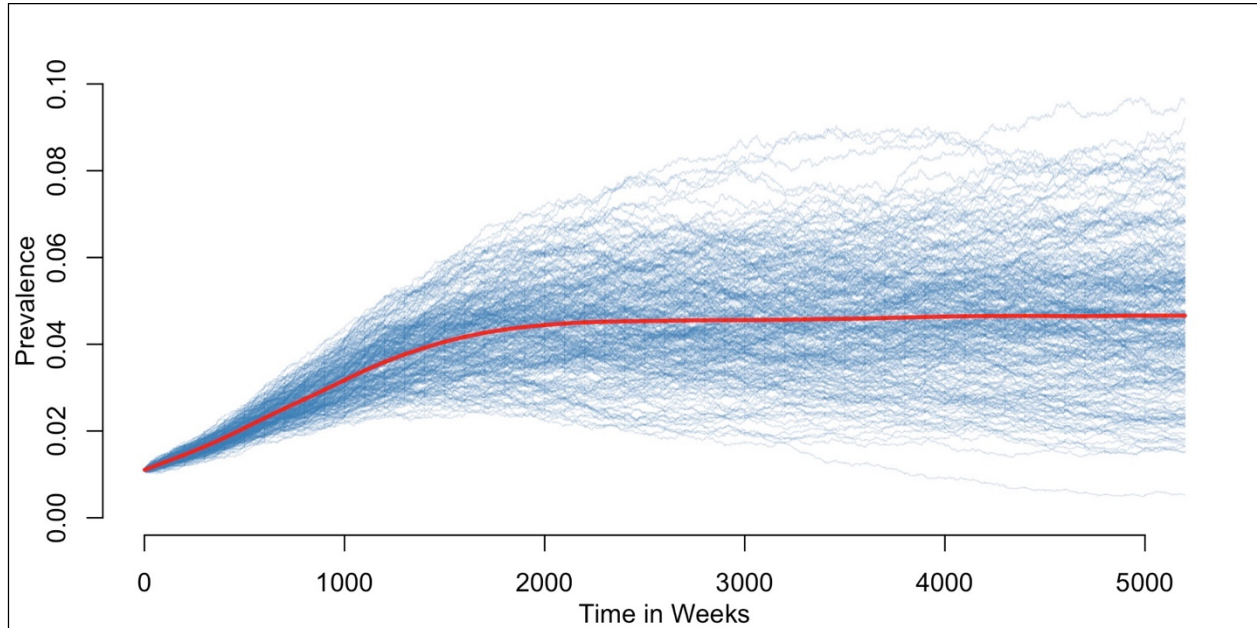
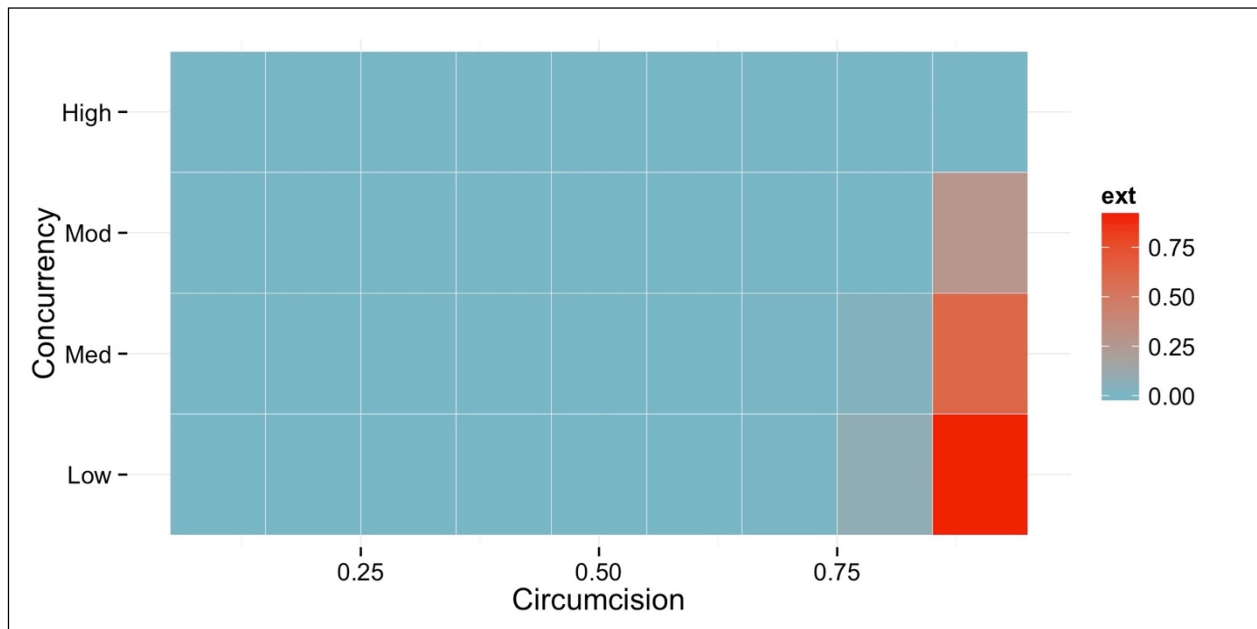


Figure S2. Probability of epidemic extinction across the 36 scenarios by concurrency and circumcision level. This probability is calculated as the proportion of simulations where the epidemic went extinct in the population.



11 REFERENCES

1. Handcock MS, Hunter DR, Butts CT, Goodreau SM, Morris M. statnet: Software Tools for the Representation, Visualization, Analysis and Simulation of Network Data. *J Stat Softw.* 2008;24(1):1548-7660.
2. Lessler J, Edmunds WJ, Halloran ME, Hollingsworth TD, Lloyd AL. Seven challenges for model-driven data collection in experimental and observational studies. *Epidemics.* 2014.
3. Cassels S, Jenness SM, Biney AAE, Ampofo WK, Dadoo FN-A. Migration, sexual networks, and HIV in Agbogbloshie, Ghana. *Demogr Res.* 2014;31:861-888.
4. Luke N, Clark S, Zulu EM. The relationship history calendar: improving the scope and quality of data on youth sexual behavior. *Demography.* 2011;48(3):1151-1176.
5. Hunter DR, Handcock MS, Butts CT, Goodreau SM, Morris M. ergm: A Package to Fit, Simulate and Diagnose Exponential-Family Models for Networks. *J Stat Softw.* 2008;24(3):nihpa54860.
6. van Duijn MA, Gile KJ, Handcock MS. A Framework for the Comparison of Maximum Pseudo Likelihood and Maximum Likelihood Estimation of Exponential Family Random Graph Models. *Soc Networks.* 2009;31(1):52-62.
7. Krivitsky PN, Handcock MS. A Separable Model for Dynamic Networks. *J R Stat Soc Ser B Stat Methodol.* 2014;76(1):29-46.
8. Carnegie NB, Krivitsky PN, Hunter DR, Goodreau SM. An approximation method for improving dynamic network model fitting. *J Comput Graph Stat.* 24(2):502-519.
9. Krivitsky PN, Handcock MS, Morris M. Adjusting for Network Size and Composition Effects in Exponential-Family Random Graph Models. *Stat Methodol.* 2011;8(4):319-339.
10. Garnett GP, Anderson RM. Factors controlling the spread of HIV in heterosexual communities in developing countries: patterns of mixing between different age and sexual activity classes. *Philos Trans R Soc L B Biol Sci.* 1993;342(1300):137-159.
11. Hunter DR, Goodreau SM, Handcock MS. ergm.userterms: A Template Package for Extending statnet. *J Stat Softw.* 2013;52(2):i02.
12. Goodreau SM, Carnegie NB, Vittinghoff E, et al. What drives the US and Peruvian HIV epidemics in men who have sex with men (MSM)? *PLoS One.* 2012;7(11):e50522.
13. Burington B, Hughes JP, Whittington WLH, et al. Estimating duration in partnership studies: issues, methods and examples. *Sex Transm Infect.* 2010;86(2):84-89.
14. Cassels S, Jenness SM, Khanna AS. Conceptual framework and research methods for migration and HIV transmission dynamics. *AIDS Behav.* 2014;18(12):2302-2313.
15. Halperin DT, Epstein H. Why is HIV prevalence so severe in southern Africa?: the role of multiple concurrent partnerships and lack of male circumcision-implications for HIV prevention: opinion. *South Afr J HIV Med.* 2007;(26):19-23,25.
16. Organization WH. *World Health Statistics 2010.* World Health Organization; 2010.

17. Mellors JW, Munoz A, Giorgi J V, et al. Plasma viral load and CD4+ lymphocytes as prognostic markers of HIV-1 infection. *Ann Intern Med.* 1997;126(12):946-954.
18. Pantazis N, Morrison C, Amornkul PN, et al. Differences in HIV natural history among African and non-African seroconverters in Europe and seroconverters in sub-Saharan Africa. *PLoS One.* 2012;7(3):e32369.
19. Eaton JW, Hallett TB. Why the proportion of transmission during early-stage HIV infection does not predict the long-term impact of treatment on HIV incidence. *Proc Natl Acad Sci.* 2014;111(45):16202-16207.
20. Fiebig EW, Wright DJ, Rawal BD, et al. Dynamics of HIV viremia and antibody seroconversion in plasma donors: implications for diagnosis and staging of primary HIV infection. *AIDS.* 2003;17(13):1871-1879.
21. Little SJ, McLean AR, Spina CA, Richman DD, Havlir D V. Viral dynamics of acute HIV-1 infection. *J Exp Med.* 1999;190(6):841-850.
22. Pilcher CD, Price MA, Hoffman IF, et al. Frequent detection of acute primary HIV infection in men in Malawi. *AIDS.* 2004;18(3):517-524.
23. Morrison CS, Chen PL, Nankya I, et al. Hormonal contraceptive use and HIV disease progression among women in Uganda and Zimbabwe. *J Acquir Immune Defic Syndr.* 2011;57(2):157-164.
24. Collini P, Schwab U, Sarfo S, et al. Sustained immunological responses to highly active antiretroviral therapy at 36 months in a Ghanaian HIV cohort. *Clin Infect Dis.* 2009;48(7):988-991.
25. Ampofo W. Current Status of HIV/AIDS Treatment, Care and Support Services in Ghana. *Ghana Med J.* 2009;43(4):142-143.
26. HIV/AIDS JUNP on. The Gap Report. *Geneva: UNAIDS.* 2014.
27. Mills EJ, Nachega JB, Buchan I, et al. Adherence to antiretroviral therapy in sub-Saharan Africa and North America: a meta-analysis. *JAMA.* 2006;296(6):679-690.
28. Chu H, Gange SJ, Li X, et al. The effect of HAART on HIV RNA trajectory among treatment-naive men and women: a segmental Bernoulli/lognormal random effects model with left censoring. *Epidemiology.* 2010;21 Suppl 4:S25-S34.
29. Hughes JP, Baeten JM, Lingappa JR, et al. Determinants of per-coital-act HIV-1 infectivity among African HIV-1-serodiscordant couples. *J Inf Dis.* 2012;205(3):358-365.
30. Wawer MJ, Gray RH, Sewankambo NK, et al. Rates of HIV-1 transmission per coital act, by stage of HIV-1 infection, in Rakai, Uganda. *J Inf Dis.* 2005;191(9):1403-1409.
31. Hollingsworth TD, Anderson RM, Fraser C. HIV-1 transmission, by stage of infection. *J Inf Dis.* 2008;198(5):687-693.
32. Jenness SM, Biney AAE, Ampofo WK, Nii-Amoo Doodoo F, Cassels S. Minimal coital dilution in Accra, Ghana. *J Acquir Immune Defic Syndr.* 2015;69(1):85-91.
33. Delva W, Meng F, Beauclair R, et al. Coital frequency and condom use in monogamous and

- concurrent sexual relationships in Cape Town, South Africa. *J Int AIDS Soc.* 2013;16:18034.
34. Keeling MJ, Rohani P. *Modeling Infectious Diseases in Humans and Animals*. Princeton University Press; 2008.
 35. Abu-Raddad LJ, Longini Jr. IM. No HIV stage is dominant in driving the HIV epidemic in sub-Saharan Africa. *AIDS.* 2008;22(9):1055-1061.
 36. Goodreau SM. Is 2 a “high number of partners”? Modeling, data, and the power of concurrency. *Sex Transm Dis.* 2013;40(1):61.
 37. Alkema L, Raftery AE, Brown T. Bayesian melding for estimating uncertainty in national HIV prevalence estimates. *Sex Transm Infect.* 2008;84 Suppl 1:i11-i16.
 38. Powers KA, Ghani AC, Miller WC, et al. The role of acute and early HIV infection in the spread of HIV and implications for transmission prevention strategies in Lilongwe, Malawi: a modelling study. *Lancet.* 2011;378(9787):256-268.